J Neuropathol Exp Neurol

Vol. 73, No. 11
November 2014
pp. 999–1008

ORIGINAL ARTICLE

Enterovirus 71 Can Directly Infect the Brainstem via Cranial Nerves and Infection Can Be Ameliorated by Passive Immunization

Soon Hao Tan, BSc, Kien Chai Ong, PhD, and Kum Thong Wong, MBBS, Mpath, FRCPath

Abstract

Enterovirus 71 (EV71)–associated hand, foot, and mouth disease may be complicated by encephalomyelitis. We investigated EV71 brainstem infection and whether this infection could be ameliorated by passive immunization in a mouse model. Enterovirus 71 was injected into unilateral jaw/facial muscles of 2-week-old mice, and hyperimmune sera were given before or after infection. Harvested tissues were studied by light microscopy, immunohistochemistry, in situ hybridization, and viral titration. In unimmunized mice, viral antigen and RNA were detected within 24 hours after infection only in ipsilateral cranial nerves, motor trigeminal nucleus, reticular formation, and facial nucleus; viral titers were significantly higher in the brainstem than in the spinal cord samples. Mice given preinfection hyperimmune serum showed a marked reduction of ipsilateral viral antigen/RNA and viral titers in the brainstem in a dose-dependent manner. With optimum hyperimmune serum given after infection, brainstem infection was significantly reduced in a time-dependent manner. A delay in disease onset and a reduction of disease severity and mortality were also observed. Thus, EV71 can directly infect the brainstem, including the medulla, via cranial nerves, most likely by retrograde axonal transport. This may explain the sudden cardiorespiratory collapse in human patients with fatal encephalomyelitis. Moreover, our results suggest that passive immunization may still benefit EV71-infected patients who have neurologic complications.

Key Words: Brainstem infections, Cranial nerves, Enterovirus 71, Passive immunization, Retrograde axonal transport, Viral transmission.

INTRODUCTION

Enterovirus 71 (EV71) is a single-stranded positive RNA virus that belongs to the family of *Picornaviridae* within the human enterovirus species A genus (1). It is one of the major causes of hand, foot, and mouth disease in children. Enterovirus 71 has reemerged in recent years to cause widespread hand, foot, and mouth disease epidemics, particularly in Asia (1, 2). Although relatively rare, EV71 infection may be complicated by serious neurologic complications such as acute flaccid paralysis and fatal encephalomyelitis. In 1997, more than 2,000 hand, foot, and mouth disease cases with 34 deaths, most likely from neurologic complications, were reported in Sarawak, Malaysia (3, 4). A year later, the largest EV71 epidemic in the Asia-Pacific region occurred in Taiwan, affecting 1.5 million people, with 405 cases of serious neurologic complications and 78 deaths (5). In 2008, in mainland China, approximately 490,000 cases with 126 deaths were reported (6). Many other countries including Japan, Singapore, Australia, Vietnam, and Cambodia experienced recurrent epidemics with fatalities either yearly or every 2 to 3 years (7–13).

Children with severe EV71 encephalomyelitis almost invariably die within a few hours of hospital admission from sudden cardiorespiratory collapse (14–17). Typically, this catastrophic terminal event is preceded by a few days of nonspecific symptoms and signs such as fever, cough, tachypnea, and lethargy, with or without skin lesions on the hand, foot, mouth, and other areas (14, 18). Autopsy studies of fatal encephalomyelitis patients have revealed extensive inflammation and damage predominantly in the spinal cord, brainstem, hypothalamus, and cerebellar dentate nucleus (15, 17–20). In the spinal cord, the anterior horns were more severely affected as compared with the posterior horns; in the brainstem, the entire medulla but only the pontine tegmentum (sparing the anterior pons) and midbrain (sparing the cerebral peduncles) were affected; very focal and mild inflammation was detected in the cerebrum, and this was more frequently found in the motor cortex (18, 21). This distinct and stereotyped distribution of inflammation has been shown in fatal cases from various countries and corresponds to the distribution of viral antigens and RNA, which were almost exclusively found within neurons in inflamed areas (15, 18–20). Based on these findings, we suggested that EV71 could enter the CNS by retrograde axonal transport in peripheral motor nerves and then spread further within the CNS by motor and nonmotor neural pathways (18).

Evidence from experimental mouse models of EV71 infection seems to support viral retrograde axonal transport up peripheral nerves (22, 23). In one of these models, we showed a stereotypic CNS distribution of virus after intramuscular injection into the murine hindlimb (23). The ipsilateral lumbar cord anterior horn motor neurons and immediate adjacent white matter axons were positive for viral antigen/RNA very

From the Department of Pathology (SHT, KTW) and Department of Biomedical Science (KCO), Faculty of Medicine, University of Malaya, Kuala Lumpur, Malaysia.

Send correspondence and reprint requests to: Kum Thong Wong, MBBS, Mpath, FRCPath, Department of Pathology, Faculty of Medicine, University of Malaya, 50603 Kuala Lumpur, Malaysia; E-mail: wongkt@ummc.edu.my

This study was supported by the Ministry of Higher Education, Malaysia Government (University of Malaya Research Grants RG141/09HTM and RG480/12HTM, Fundamental Research Grant FP021/09, and High Impact Research Grant H20001-E00004).

The authors declare no conflict of interest.

soon after infection. Later, the motor trigeminal nucleus in the brainstem and motor cortex were also found to be infected. Based on these findings, we hypothesized that the virus may be able to use not only the motor components of spinal nerves but also cranial nerves to enter the CNS (18, 23). Here, we used the same mouse model of encephalomyelitis to investigate the possibility that EV71 could directly infect the brainstem via cranial nerves. Rapid and severe neuronal infection in the brainstem could help explain the sudden catastrophic onset of cardiorespiratory collapse in patients with fatal encephalomyelitis (24, 25).

At present, there are no effective antiviral drugs or licensed vaccines available for severe EV71 infections (26, 27). We and others have previously shown that hyperimmune sera containing neutralizing antibodies were able to protect experimentally infected mice from disease (28–31). Moreover, intravenous immunoglobulins have been used prophylactically and therapeutically against enterovirus infection in neonates and immunocompromised adults and have been shown to reduce mortality (32–36). Although intravenous immunoglobulins have also been used extensively in EV71 outbreaks, the mechanism of action is not well understood, but neutralizing antibodies may play a role (37). After infection, passive immunization with neutralizing antibodies has been found to improve survival in mice (28–30), but so far, it has not been clearly demonstrated if it is effective in established CNS infection. To evaluate the potential usefulness of hyperimmune serum containing specific neutralizing antibodies as a therapeutic option, in relation to CNS infection, we also investigated passive immunization before and after brainstem involvement.

MATERIALS AND METHODS

Virus Stock

African green monkey kidney (Vero) cells grown and maintained in Dulbecco modified Eagle medium supplemented with 5% fetal bovine serum were used for virus stock preparation, titration, and microneutralization assays. The mouse-adapted EV71 strain (MAVS) used throughout the study was prepared, titrated, and concentrated as previously described (23, 38).

Preparation of Hyperimmune Serum

Hyperimmune serum with neutralizing antibodies against MAVS was prepared by injecting formaldehyde-inactivated virus vaccine into mice, as previously described (31). Briefly, 6- to 8-week-old ICR outbred mice were immunized by the intraperitoneal route with a dose of 16 μg of vaccine containing 0.5 mg/mL aluminum hydroxide as adjuvant. First and second boosters containing the same doses were given at 14 and 28 days after primary immunization, respectively. Mock-immunized mice as negative controls were given the same concentration of formaldehyde-fixed Vero cell lysates. The mice were killed 3 days after the second booster, and sera were collected and tested for neutralizing antibodies using a microneutralization test as previously described (31).

Testing Effectiveness of Hyperimmune Serum for Passive Immunization

Hyperimmune serum with neutralizing titer of 1/512 against MAVS was used for passive immunization in all experiments. Preliminary testing of its effectiveness to ameliorate infection when given before MAVS infection was done at various doses (volume range, 25–225 μL) and timing (range, 2–16 hours before infection). The aim was to find a dose and timing that could abrogate viremia and viral infection in noninjected muscle groups (thigh and limb muscles) after intramuscular injection into the unilateral jaw/facial muscles, as described in Experiment 1. A dose of 100 μL hyperimmune serum given 4 hours before infection was able to achieve this end point.

Animal Infection Experiments

Altogether, 4 sets of infection experiments on 2-week-old ICR mice were performed. All experiments were approved by the University of Malaya Animal Welfare and Use Committee and performed according to its guidelines.

In Experiment 1 (n = 24), CNS infection without passive immunization after intramuscular injection into unilateral jaw/facial muscles was investigated. Using a 31-guage needle, a dose of 6.3×10^5 $CCID_{50}$ MAVS in 10 μL was delivered into each mouse, and the mice were then observed for 72 hours. Eight animals each were killed at 24, 48, and 72 hours postinfection (hpi), respectively. At each time point, tissues were harvested from 4 animals for pathologic analysis and the other 4 animals for virus titration. Mock-infected control mice (n = 8) were injected with phosphate buffered saline and killed at 72 hpi.

In Experiment 2 (n = 24), a single dose of 100 μL (designated ''low-dose'') hyperimmune serum was injected intraperitoneally into each mouse 4 hours before infection, as described in Experiment 1. Again, 8 animals each were killed at 24, 48, and 72 hpi, respectively, and tissues were harvested as before. Mock-immunized control mice (n = 8) received serum from mice previously immunized only with formaldehyde-fixed Vero cell lysates and were killed at 72 hpi.

In Experiment 3, 3 groups of 8 animals each were intraperitoneally injected with a single dose of 200-μL (designated ''high-dose'') hyperimmune serum 4 hours before infection and at 12 hpi and 24 hpi. This dose was the maximum volume possible because of the small peritoneal cavity of a 2-week-old mouse. Infection was as described in Experiment 1. A control group (n = 8) was mock treated at 12 hpi, receiving Vero cell lysate-derived serum. All mice were killed at 72 hpi for either pathologic analysis (n = 4) or virus titration (n = 4) from each group.

Finally, in Experiment 4, the overall survival of mice receiving a single high dose of hyperimmune sera preinfection (n = 4) and at 12 hpi (n = 4) and 24 hpi (n = 4), respectively (similar to Experiment 3), was assessed for a longer period of 21 days. Four control animals prepared as in Experiment 3 were used for comparison.

Histopathology

All tissues were fixed and routinely processed as previously described (23). Briefly, after 10% neutral buffered formalin fixation, each animal was cut transversely to obtain 7 standard tissue blocks of the whole animal so that most major organs could be examined. Tissue blocks were decalcified in 5% formic acid overnight and routinely processed. Four-micrometer-thick sections from each block were stained with hematoxylin and eosin and examined by immunohistochemistry

(IHC) and in situ hybridization (ISH), respectively. For each CNS tissue block, 3 to 5 sections were initially stained with hematoxylin and eosin and examined by IHC. When the anatomic sites of interest (e.g. motor trigeminal nucleus) was identified in the tissue sections, at least 2 additional adjacent sections were used for ISH.

Immunohistochemistry

Immunohistochemistry was performed as previously described (23). Briefly, tissue sections were dewaxed and rehydrated in graded ethanols. Antigen retrieval was performed by boiling in citrate buffer (pH 6) at 99°C for 20 minutes. The primary antibody, polyclonal rabbit anti-EV71, was incubated for 2 hours at room temperature, followed by standard secondary antibody linkage and 3,3′-diaminobenzidine substrate development (18, 23). The sections were counterstained with Harris hematoxylin. Tissues from EV71-infected mouse served as positive controls; normal healthy mouse tissues served as negative controls.

In situ hybridization

In situ hybridization was performed as previously described (23). After dewaxing and rehydration as for IHC,

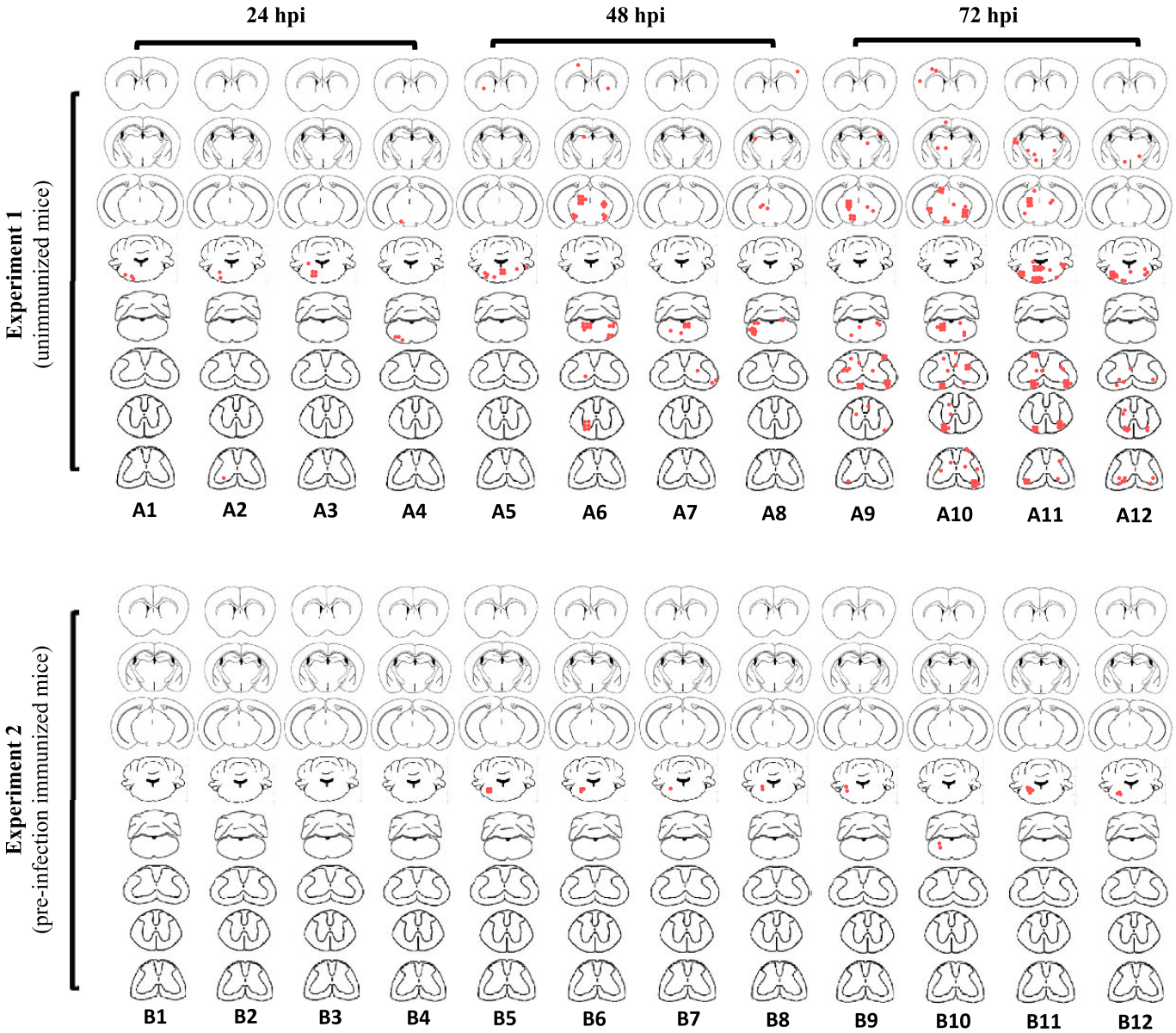

FIGURE 1. Approximation of the distribution of Enterovirus 71 antigen/RNA or damaged neurons in the CNS after unilateral jaw/facial muscle infection in Experiment 1 (unimmunized mice, A1–A12) and Experiment 2 (preinfection immunized mice, B1–B12). Mice in Experiment 1 (A1–A4) showed ipsilateral brainstem involvement at 24 hours postinfection (hpi) and bilateral involvement at 48 hpi (A5–A12). In Experiment 2, mild ipsilateral brainstem involvement was observed only at 48 hpi (B5–B12). Each red dot represents the equivalent of a positive or damaged neuron or white matter axon. Cross sections of cerebral cortex, diencephalon/cortex, midbrain/cortex, caudal pons/medulla/cerebellum, medulla/cerebellum, cervical, thoracic, and lumbar spinal cords are displayed for each mouse.

tissue sections were treated with hydrochloric acid and proteinase K at 37°C for 20 minutes. Approximately 1 ng of digoxigenin-labeled DNA probe (targeting the 5-nontranslated region of EV71 genome) in hybridization buffer was heated at 110°C for 12 minutes, followed by incubation at 42°C for 16 hours. Anti-digoxigenin antibody conjugated with alkaline phosphatase (Roche, Mannheim, Germany) was added followed by nitroblue tetrazolium/5-bromo-4-chloro-3-indolyl phosphate substrate and incubated in the dark for 16 hours. The sections were counterstained with Mayer hematoxylin. Similar positive and negative controls in the IHC procedure were used.

Viral Titration

From each animal, the whole brainstem, ''upper'' spinal cord (upper half), ''lower'' spinal cord (lower half), serum, and pooled muscles from bilateral forelimbs and thighs were collected for viral titration. Cerebral tissues were not titrated for virus because preliminary results showed negligible viral antigen/RNA present. Cross contamination between animals and tissue types was minimized using different dissection sets and careful handling. Each organ/tissue was weighed, and 10% homogenate (wt/vol) was prepared using Dulbecco modified Eagle medium supplemented with 2% fetal bovine serum. Viral titers were determined using $CCID_{50}$ and calculated using the Karber method as previously described (23). Viral titers from each organ/tissue were pooled and presented as average titer (mean) with SEM.

Statistical Analysis

Viral titers were analyzed using Kruskal-Wallis test to determine any differences across all tissue types. The Mann-Whitney U test was used to determine if any 2 tissue types were different. A value of $p < 0.05$ was considered significant.

RESULTS

Experiment 1: Infection Without Passive Immunization

In Experiment 1, infected mice started to show signs of disease such as hunching of the back, ruffled fur, and obvious paralysis in both hindlimbs at 60 hpi; these signs became more severe at 72 hpi. The presence of jaw or facial muscle paralysis was difficult to determine. The mock-infected control mice were all healthy and active throughout the experiment.

In all 4 mice killed at 24 hpi, viral antigens and RNA could already be detected by IHC and ISH, respectively, in CNS and skeletal muscles. The approximate topographic distributions of neuronal viral antigen/RNA or damaged neurons in CNS tissues in each mouse are shown in Figure 1 (Mice A1–A4). In the brainstem, viral antigen and RNA were beginning to be detected in the motor trigeminal nucleus, reticular formation, and facial nucleus, ipsilateral to the injection site only. In addition, viral antigen/RNA was also found within ipsilateral cranial nerves in all animals (Fig. 2A, B). An ipsilateral single anterior horn motor neuron in the lumbar spinal cord of 1 mouse was found to be infected (Mouse A2, Fig. 1). All CNS neurons appeared normal by light microscopy, with no obvious surrounding inflammation.

At the site of injection, numerous fibers in the jaw/facial muscles were positive for viral antigen/RNA. In contrast, only a few fibers in the contralateral jaw/facial muscles were positive. Elsewhere in the tongue, head, and limbs, focal and scant viral antigen/RNA positivity was detected in a few muscle fibers bilaterally. All other tissues were negative.

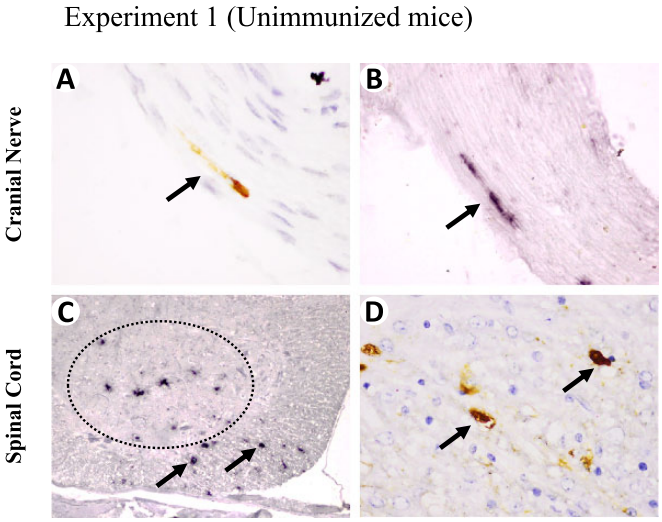

FIGURE 2. Pathologic findings in Enterovirus 71 (EV71)–infected mice in unimmunized animals (Experiment 1). **(A–D)** In all the animals, viral antigens **([A]** arrow**)** and RNA **([B]** arrow**)** were found in cranial nerves. In the spinal cord, at 72 hours postinfection (hpi), viral RNA **([C]** arrows**)** and antigens **([D]** arrows**)** were often detected in white matter axons adjacent to anterior horn cells that were positive for viral antigens or RNA **([C]** circle**)**. Immunohistochemistry with DAB chromogen and hematoxylin counterstain **(A, D)**. In situ hybridization with hematoxylin counterstain **(B, C)**. Original magnification: 60× objective **(A)**; 40× objective **(B, D)**; 10× objective **(C)**.

In animals killed at 48 hpi, the distribution of neuronal viral antigen/RNA or damaged neurons in the brainstem was similar to those at 24 hpi except for bilateral involvement (Fig. 1, Mice A5–A8). Moreover, more neurons were involved in the motor trigeminal nuclei (Fig. 3A–D), reticular formation (Fig. 3F), and facial nuclei (Fig. 3E). A few neurons in the bilateral thalamus, hypothalamus, motor cortex, and red nucleus also became involved. Viral antigen/RNA was found within cranial nerves in all animals. In the spinal cord, neuronal infection mainly involved unilateral anterior horn cells in 2 of the mice (Fig. 1, Mice A6 and A7). Infected neurons showed neuronal vacuolation and damage (Fig. 3A). Axons in the white matter immediately adjacent to infected anterior horn cells at or near the site where peripheral motor nerves usually exit were positive for viral antigen/RNA (Fig. 2C, D). Overall, no obvious inflammation was observed.

Muscle fibers at the injection site demonstrated extensive and dense viral antigen/RNA, marked inflammation, and necrosis. Other skeletal muscles (including limb muscles) and brown adipose tissues showed some viral antigen/RNA bilaterally with minimal inflammation.

In animals killed at 72 hpi, there were similar distributions of neuronal viral antigen/RNA or neuronal damage in the CNS with even more extensive bilateral involvement of the brainstem compared with 48 hpi (Fig. 1, Mice A9–A12).

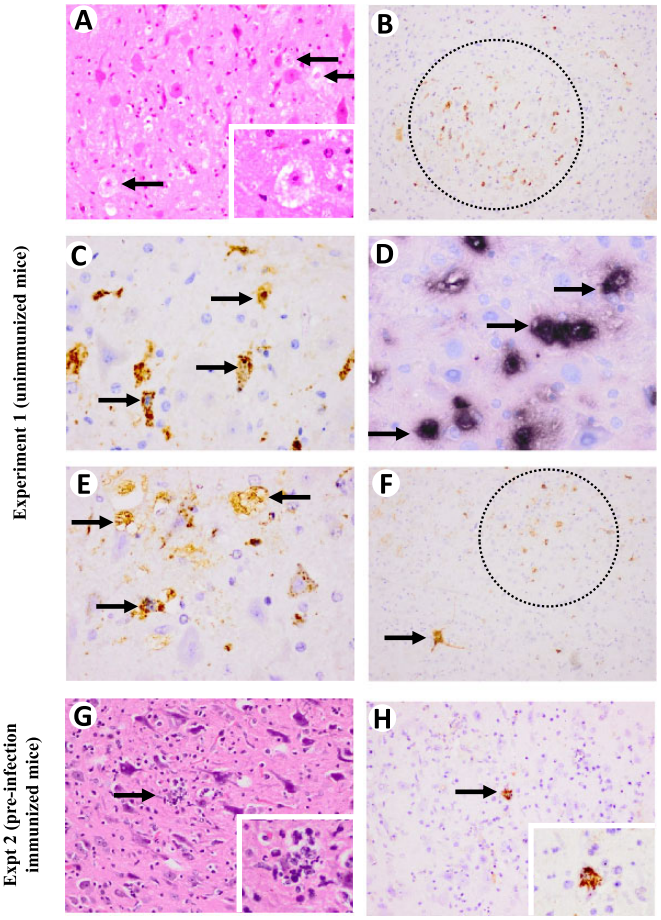

FIGURE 3. (A–H) Pathologic findings in Enterovirus 71 (EV71)–infected mice in unimmunized animals **(**Experiment 1**[A–F])** and preinfection immunized animals **(**Experiment 2 **[G, H])**. Infected neurons in the motor trigeminal nucleus showed degeneration and necrosis, with no obvious inflammation **([A]** arrows, inset**)**, viral antigens **([B]** circle; **[C]** arrows**)**, and viral RNA **([D]** arrows**)**. Viral antigens were also detected in the facial nucleus **([E]** arrows**)**, reticular formation **([F]** circle**)**, and gigantocellular reticular nucleus **([F]** arrow**)**. In Experiment 2, neuronal necrosis and very mild inflammation **([G]** arrow, inset**)** and very focal viral antigens **([H]** arrow, inset**)** were detected in the motor trigeminal nucleus. Hematoxylin and eosin stain **(A, G)**. Immunohistochemistry with DAB chromogen and hematoxylin counterstain **(B, C, E, F, H)**. In situ hybridization with hematoxylin counterstain **(D)**. Original magnification: 40× objective **(C, D, E** and all insets**)**; 20× objective **(A, G, H)**; 10× objective **(B, F)**.

Additional bilateral regions that showed positive neurons included the lateral cerebellar nucleus (dentate nucleus), gigantocellular reticular nucleus, solitarius nucleus, nucleus ambiguous area, and motor and sensory cortices. Again, cranial nerves were positive for viral antigen/RNA in all animals. In the spinal cord, neurons in the anterior, intermediate, and posterior horns were involved bilaterally, although cells in the intermediate and posterior horns appeared to show less infection than anterior horn cells. The degrees of ipsilateral and contralateral spinal cord involvement were similar (Fig. 1, Mice A9–A12). Overall, no obvious inflammation was observed.

Viral antigen/RNA in skeletal muscles and adipose tissues was found to be more extensive and in higher concentrations compared with 48 hpi. Viral antigen/RNA was not detected in lung or heart tissues in any mouse in Experiment 1, and both tissues appeared histologically normal, with no evidence of pulmonary edema, pneumonia, or myocarditis.

Viral titers in the whole brainstem, ''upper'' and ''lower'' spinal cord segments, and serum are shown in Figure 4. Compared with both ''upper'' and ''lower'' spinal cords, brainstem viral titers at 24 and 48 hpi were significantly higher ($p < 0.05$) (Fig. 4). Mean viral titers in the brainstem at 24, 48, and 72 hpi were log $CCID_{50}$ 2.56, 3.63, and 3.63, respectively. Brainstem viral titer at 24 hpi was significantly lower than 48 hpi and 72 hpi ($p < 0.05$). As early as 24 hpi, serum showed the highest viral titer that increased across time. Viral titers in pooled muscles increased from 24 to 72 hpi.

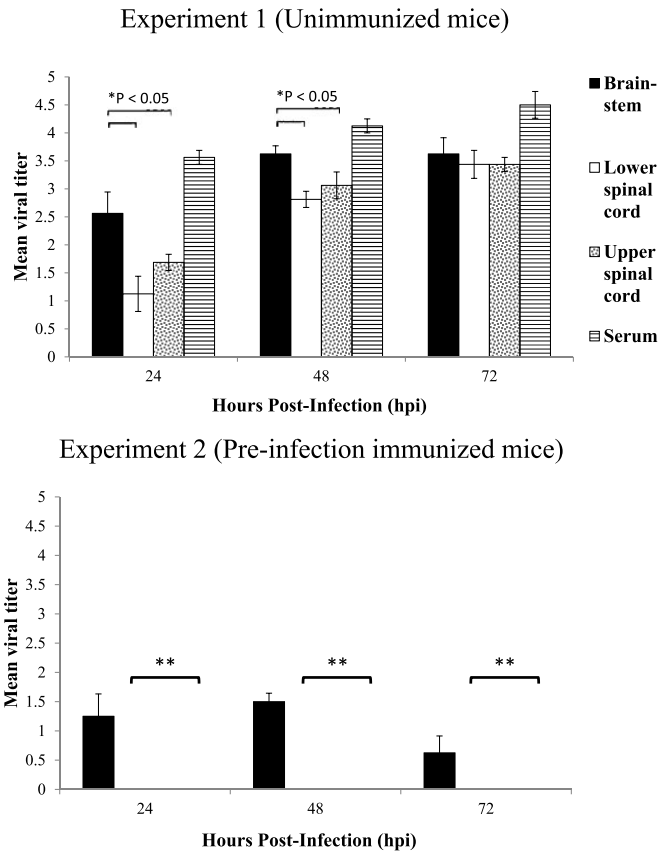

FIGURE 4. Enterovirus 71 titers in CNS tissues (n = 4 for each type) and sera from unimmunized animals (Experiment 1) and preinfection immunized (Experiment 2) mice killed at 24, 48, and 72 hours postinfection (hpi). In Experiment 1, brainstem viral titer was significantly higher than ''lower'' spinal cord and ''upper'' spinal cord at 24 hpi and at 48 hpi, respectively. In Experiment 2, viral titers were detectable in the brainstem but were below detection (**) in spinal cords and serum at 24, 48, and 72 hpi. Mean viral titers are expressed as the log $CCID_{50}$ ± SEM.

Experiment 2: Low-Dose Preinfection Passive Immunization

In Experiment 2, none of the 24 mice that were given passive immunization 4 hours before MAVS infection showed any signs of disease. Mock-immunized control animals (n = 8) showed similar signs of disease as in Experiment 1. At 24 hpi, there was no evidence of infection in the CNS (Fig. 1, Mice B1–B4) or other tissues, except for positive viral antigen/RNA in a few fibers in the injected muscle only. At 48 hpi, there was only minimal neuronal viral antigen/RNA or damaged neurons that were limited to the ipsilateral brainstem, (Fig. 1, Mice B5–B8) in the motor trigeminal nucleus and reticular formation but not the facial nucleus. The intensity of IHC/ISH staining (Fig. 3H) was very much lower compared with the corresponding areas in mice from Experiment 1 (Fig. 3H); only occasional very focal and mild inflammation was observed. Inflammatory cells consisted mainly of neutrophils and macrophages (Fig. 3G). Moreover, there was no evidence of viral antigen/RNA in the spinal cord or other brain regions outside the brainstem. Only focal sparse viral antigen/RNA was detected in the injected muscle. All other muscles and non-CNS tissues were negative. Similar findings were obtained in animals killed at 72 hpi (Fig. 1, Mice B9–B12). Mock-immunized control animals showed infection similar to mice in Experiment 1.

The mean viral titers in the brainstem in Experiment 2 at 24, 48, and 72 hpi were log $CCID_{50}$ 1.25, 1.5, and 0.625, respectively (Fig. 4). Thus, viral titers did not significantly change across time, as in Experiment 1. More importantly, there was a significant reduction ($p < 0.05$) of brainstem viral titers at all comparable time points. The viral titers in the ''upper'' and ''lower'' spinal cords, serum, and pooled muscles were below detection levels (Fig. 4). Overall, mean viral titers in Experiment 2 were all significantly lower than those in Experiment 1 at all time points for all tissue types ($p < 0.05$). Mock-immunized control mice showed viral titers similar to those in infected mice in Experiment 1.

Experiment 3: High-Dose Preinfection and Postinfection Passive Immunization

In Experiment 3, 3 groups of mice received high-dose (200 μL) hyperimmune serum at 4 hours preinfection and at 12 hpi and 24 hpi by MAVS, respectively. Tissues from 4 mice in each of the 3 treated groups killed at 72 hpi were analyzed. Viral antigen/RNA was not detected in the CNS (Fig. 5), muscles, or other tissues in the mice that received high-dose preinfection hyperimmune serum.

Animals given high-dose hyperimmune serum at 12 hpi showed very focal neuronal viral antigen/RNA or neuronal damage exclusively in the brainstem (Fig. 5), involving bilateral motor trigeminal nuclei (Fig. 6A), reticular formation, and facial nuclei. In the group treated at 24 hpi, the animals showed similar involvement (Fig. 5), except for a slightly higher density of viral antigen/RNA (Fig. 6C). Overall, neuronal viral antigen/RNA or neuronal damage in the CNS was much less in the 2 postinfection treated groups compared with the mock-treated controls (Figs. 5, 6). Infected neurons showed vacuolation, with no obvious surrounding inflammation.

Skeletal muscles throughout the body were extensively infected in all animals, with the controls being the most severely affected, followed by mice treated at 24 hpi and 12 hpi (Fig. 6B, D, F). In general, the mock-treated control mice showed similar infection to mice in Experiment 1.

Viral titers from CNS tissues and sera in the postinfection treated groups and mock-treated control mice for Experiment 3

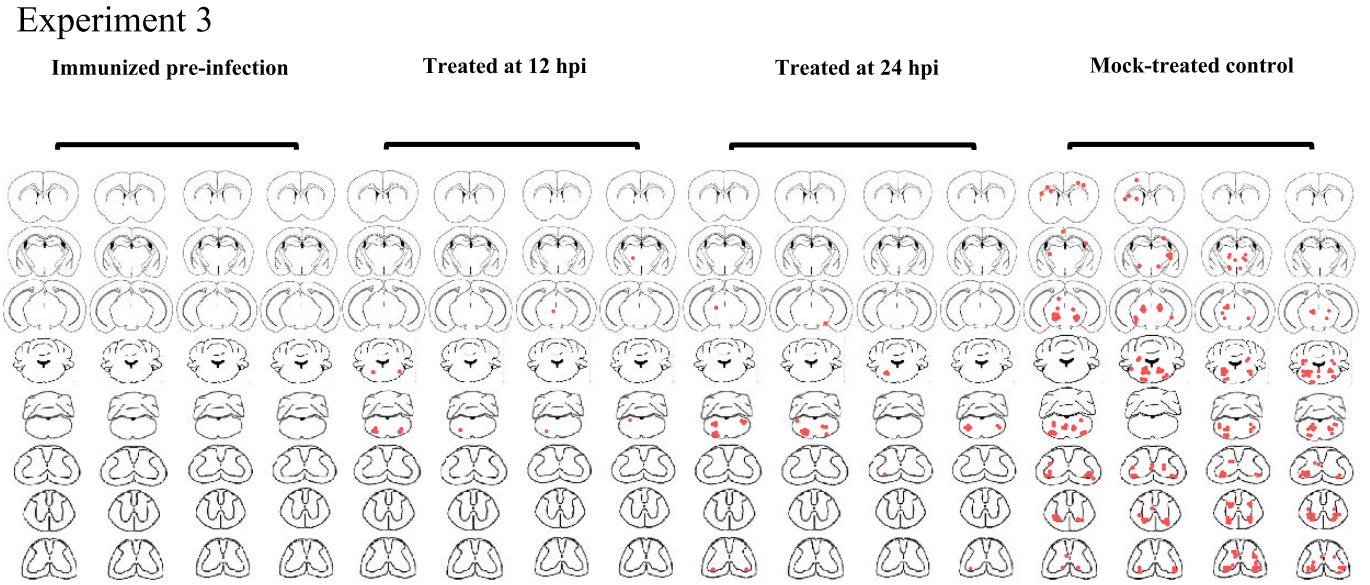

FIGURE 5. Approximation of the distribution of viral antigen/RNA or damaged neurons in the CNS in all animals killed at 72 hours postinfection (hpi) in Experiment 3. In the groups treated at 12 and 24 hpi, the brainstem was much less involved compared with the mock-treated group. The preinfection immunized mice were totally protected. Each red dot represents the equivalent of a positive or damaged neuron or white matter axon. Cross sections of cerebral cortex, diencephalon/cortex, midbrain/cortex, caudal pons/medulla/cerebellum, medulla/cerebellum, and cervical, thoracic, and lumbar spinal cords are displayed for each mouse.

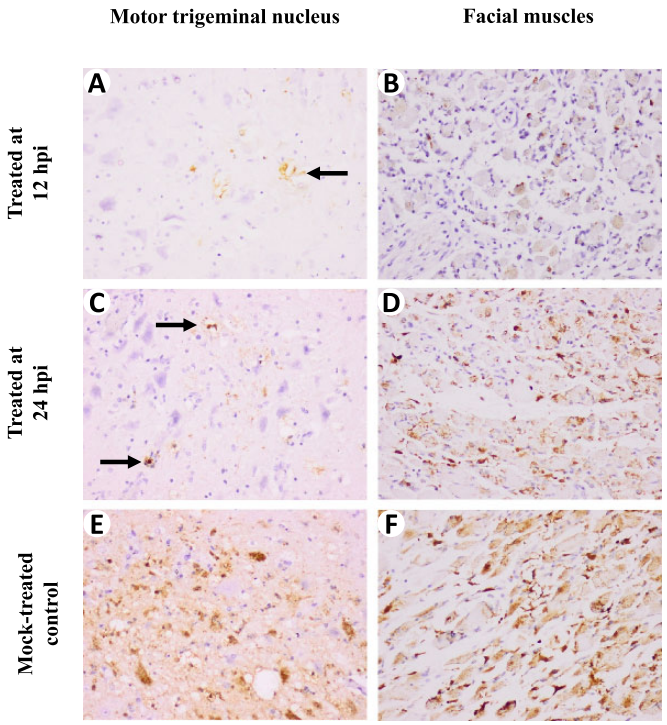

FIGURE 6. Pathologic findings in Enterovirus 71 (EV71)–infected mice in Experiment 3 killed at 72 hours postinfection (hpi). Minimal viral antigens in the motor trigeminal nucleus in infected animals treated at 12 hpi **(A)** and 24 hpi **(C)** compared with dense viral antigens in mock-treated control animals **(E)**. The distribution of viral antigens in facial muscles is similar between these treated groups **(B, D)**, although the density is generally lower than in mock-treated control animals **(F)**. Original magnification: 20× objective **(A–F)**.

are shown in Figure 7. Overall, viral titers in the brainstem and spinal cords in the treated groups were significantly lower than those in the mock-treated control group ($p < 0.05$) (Fig. 7).

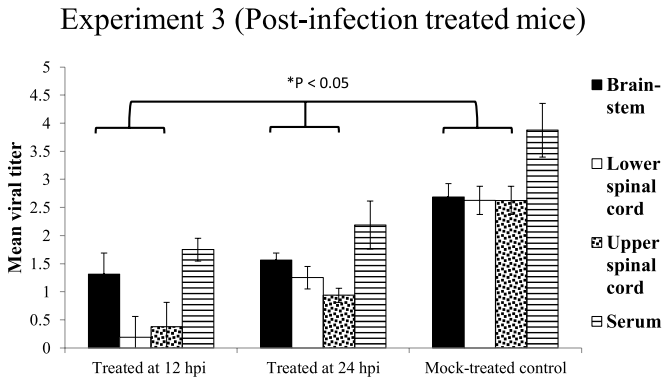

FIGURE 7. Viral titers in CNS tissues (n = 4 for each tissue type) and sera from infected animals treated at 12 and 24 hours postinfection (hpi) and mock-treated control animals killed at 72 hpi in Experiment 3. Viral titers were all significantly lower ($p < 0.05$) in the groups treated at 12 hpi and 24 hpi versus the controls for all the different types of CNS tissues, respectively. Mean viral titers are expressed as log $CCID_{50}$ ± SEM.

Furthermore, viral titers in the group treated at 12 hpi were lower than those in the group treated at 24 hpi, although the difference was only significant for the ''upper'' spinal cord and the ''lower'' spinal cord ($p < 0.05$). In all tissues from mice receiving high-dose preinfection hyperimmune serum, viral titers were below detection level, except for the brainstem of 1 mouse (out of 4 mice), which showed a low titer of log $CCID_{50}$ 0.25. Viral titers in pooled muscles were lowest in the 12 hpi group, with increasing titers in the 24 hpi group and control mice.

Experiment 4: High-Dose Preinfection and Postinfection Passive Immunization and Survival

In Experiment 4, all mice receiving high-dose hyperimmune serum at 4 hours preinfection (n = 4) did not show any signs of disease during the entire 21-day observation period (Fig. 8). Two out of the 4 mice that received hyperimmune sera at 12 hpi showed ruffled fur and weight loss, with no observable paralysis from Day 8 onward and died on Day 13. Two out of the 4 mice that received hyperimmune sera at 24 hpi showed ruffled fur and mild paralysis of one hindlimb from 72 hpi onward and died on Day 10. One additional mouse from this group showed only weight loss from Day 6 onward and died on Day 11. The mock-treated control mice (n = 4) all showed signs of disease as described in Experiment 1 and died on Day 4 (Fig. 8).

DISCUSSION

We have previously shown that EV71 is able to enter and infect the murine spinal cord by retrograde axonal transport via peripheral spinal motor nerves after unilateral intramuscular injection into the hindlimb (23). In the current study, we have demonstrated that EV71 is also able to enter and directly infect the murine brainstem via cranial nerves, most likely also by retrograde axonal transport. Viral spread into the ipsilateral CNS occurred as early as 24 hpi (Experiment 1), as evidenced by the detection of viral antigen/RNA in the cranial nerves

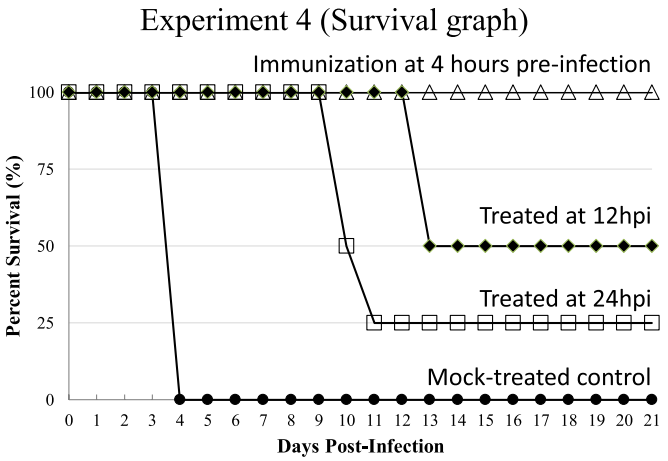

FIGURE 8. Survival graph of infected animals in mock-treated, 12 hours postinfection (hpi)–treated, 24 hpi–treated, and preinfection immunized groups (n = 4 each group) followed for 21 days. Treated mice showed improved survival, whereas all mock-treated animals died. Preinfection immunized mice all survived.

(Fig. 2), motor trigeminal nucleus, reticular formation, and facial nucleus (Fig. 3). Furthermore, at 24 and 48 hpi, viral titers in the brainstem were significantly higher than those in the spinal cord (Fig. 4). After unilateral viral infection of the ipsilateral jaw/facial muscles, viruses were presumed to have crossed the neuromuscular junctions to enter distal motor nerve terminals to travel up the fifth and seventh cranial nerves to infect the motor trigeminal nucleus and facial nucleus, respectively.

From 48 hpi onward (Experiment 1), viral spread into the CNS seems to be more complicated, that is, viral antigen/RNA in the contralateral motor neurons of the brainstem and spinal cord began to appear. We postulate that, as early as 24 hpi, viremia disseminated viruses to other skeletal muscles after viral replication in injected muscles and/or leakage therefrom (23). Infection of other and bilateral muscle groups would then enable virus to enter the brainstem and spinal cord by spreading up the respective nerves innervating these muscles. That viremia plays a significant role in systemic virus spread was clearly shown in Experiment 2 in which abrogation of viremia resulted in infection of the ipsilateral brainstem and injected muscles only.

In unimmunized animals, the reticular formation around the motor trigeminal and facial nuclei and the entire medulla, including the gigantocellular reticular nucleus, lateral reticular nucleus, solitarius nucleus, and the nucleus ambiguous, became severely involved (Experiment 1). Infection of the reticular formation is most likely via the rich and extensive neuronal interconnections with the motor trigeminal and facial nuclei (39–41). Although we did not demonstrate direct medullary infection via retrograde viral transmission up cranial nerves ninth to 12th, our findings suggest that involvement of the fifth and seventh cranial nerves and their respective motor nuclei was sufficient to lead to medullary infection. Thus, similar involvement of medullary cardiorespiratory centers via cranial nerves could cause the sudden collapse typically observed in patients with fatal encephalomyelitis (24, 25, 42, 43). Indeed, we believe that viral transmission in cranial nerves plays a critical role in the cause of sudden death. Damage to the medulla could lead to very high levels of norepinephrine and epinephrine that may cause cardiac damage and arrhythmia and pulmonary edema via raised pulmonary vascular pressures (neurogenic pulmonary edema) (17, 44). We did not attempt to infect muscles supplied by the ninth to 12th cranial nerves by intramuscular injection because of the technical difficulties of handling small muscle groups in 2-week-old mice. Besides the severe neuronal destruction in the brainstem, it is possible that myositis might also contribute to death in the model. On the other hand, myositis has not been demonstrated in human EV71 encephalomyelitis (18, 45).

''Cytokine storm'' may also play a role in the terminal events of fatal encephalomyelitis because several human studies found raised cytokines including interleukin-1β (IL-1β), IL-6, IL-10, IL-13, and interferon-γ to be associated with pulmonary edema in fatal encephalomyelitis. These inflammatory cytokines were thought to increase pulmonary vascular permeability, leading to pulmonary edema and death (46–48). Interestingly, pulmonary edema was not observed in any of the animal models described so far, including the current study (49). Based on our findings, we believe that direct brainstem infection is as important, if not more important than cytokine storm–induced pulmonary edema/functional dysregulation as a cause of death. Further investigations are needed to confirm this.

Previously, we and others have demonstrated that preinfection passive immunization with neutralizing antibodies protected EV71-infected mice from paralysis and death (28–31, 50). Moreover, postinfection immunization studies have also demonstrated improved survival (28–30). However, in all these studies, CNS tissues were not examined for evidence of infection before or after passive immunization/treatment. In the present study, a single low-dose preinfection hyperimmune serum had significantly reduced infection in the brainstem and other tissues examined, as evidenced by a marked reduction of viral antigen/RNA and viral titers (Figs. 1, 4) and observed clinical improvement. Furthermore, mice that received high-dose preinfection hyperimmune sera in Experiment 3 were totally protected (Fig. 5). Hence, there was a positive dose response to hyperimmune sera.

The results of postinfection treatments obtained in Experiments 3 and 4 clearly showed that, even in relatively advanced EV71 infections with neurologic complications, hyperimmune sera was still beneficial. Even with a single dose of hyperimmune serum, brainstem infection was significantly ameliorated, with a reduction of viral antigen/RNA and viral titer in the tissues if treatment was given within 24 hpi. Furthermore, Experiment 4 showed improved survival in treated mice observed for a 21-day period. In addition, signs of disease were less severe, appeared later, and in fewer mice compared with mock-treated controls. Thus, effective hyperimmune serum seems to be able to control and ameliorate CNS infection in a dose- and time-dependent manner. Better results may be possible with multiple postinfection doses of hyperimmune sera. Overall, our findings provide a better rationale and a firmer basis for the current empirical use of intravenous immunoglobulins and neutralizing antibodies in severe human EV71 infections (37, 51, 52).

The effectiveness of hyperimmune serum to ameliorate infection is probably directly related to its anti-EV71 neutralizing antibodies. Certainly, neutralizing antibodies were most likely involved in eliminating viremia if given in adequate doses and before infection (Experiments 2, 3). The antibodies could theoretically reduce neuronal infection, first reducing retrograde axonal transport, by eliminating viruses in infected neurons and by preventing viral spread to other CNS neurons. Whether these antibodies were involved in virus elimination from infected neurons or prevention of virus spread in the CNS parenchyma is uncertain because it is well known that macromolecules such as antibodies do not penetrate the blood-brain barrier (53). However, alteration of blood-brain barrier permeability as a result of proinflammatory cytokines such as tumor necrosis factor, IL-1β, and IL-6 could allow neutralizing antibodies to enter the CNS parenchyma (53). Alternatively, the immature blood-brain barrier in 2-week-old mice may facilitate movement of antibodies into the parenchyma (54, 55). Apart from antibodies, the hyperimmune serum may contain factors associated with cell-mediated immunity that might help eliminate infection (56).

The possibility of antibody-dependent enhancement of EV71 infection with passive immunization has been investigated,

and results showed that antibody-dependent enhancement was associated with subneutralizing antibodies (57, 58). In our experiments, there was no apparent antibody-dependent enhancement in the immunized/treated animals perhaps because our hyperimmune serum had a high neutralizing antibody titer (57, 58). Further efforts are needed to understand the host immune responses and the mechanisms involved in infection control by passive immunization, in particular, the role of neutralizing antibodies.

Recent evidence suggests that EV71 may enter the body via tonsillar crypt epithelium (45), giving rise to viremia and facilitation of viral entry into neuromuscular junctions or nerve terminals found in skeletal muscles, or entry into the peripheral nerve directly, resulting in retrograde motor nerve transmission into the brainstem and spinal cord (23, 45, 59). This hypothesis is consistent with the stereotyped topographic distribution of inflammation and virus in the human CNS (18, 21) and supported by findings in our model (23). We have also previously shown that our mouse model could be orally infected to produce similar CNS infection, albeit less consistently, than by intramuscular injection (23). Although intramuscular injection does not represent the natural infection route, we believe it could be used to model retrograde peripheral nerve transmission and viral entry into the CNS. Hence, our mouse model remains valid and useful for gaining further insight into EV71 neuropathogenesis. Nonetheless, our findings should be confirmed in more recently described transgenic mouse models of EV71 infection (59, 60).

In conclusion, we have demonstrated that EV71 is able to enter and infect the murine brainstem most likely by retrograde axonal transport in the motor components of cranial nerves. Within the brainstem, the reticular formation could facilitate viral spread from the motor trigeminal and facial nuclei into the medulla to cause cardiorespiratory collapse. Central nervous system infection can be significantly ameliorated by hyperimmune sera containing neutralizing antibodies, suggesting that there may still be a window of opportunity for therapeutic intervention after the onset of neurologic complications.

REFERENCES

1. Solomon T, Lewthwaite P, Perera D, et al. Virology, epidemiology, pathogenesis, and control of enterovirus 71. Lancet Infect Dis 2010;10:778–90
2. Wong KT. Emerging and re-emerging epidemic encephalitis: A tale of two viruses. Neuropathol Appl Neurobiol 2000;26:313–18
3. Cardosa MJ, Krishnan S, Tio PH, et al. Isolation of subgenus B adenovirus during a fatal outbreak of enterovirus 71-associated hand, foot, and mouth disease in Sibu, Sarawak. Lancet 1999;354:987–91
4. Chan LG, Parashar UD, Lye MS, et al. Deaths of children during an outbreak of hand, foot, and mouth disease in Sarawak, Malaysia: Clinical and pathological characteristics of the disease. For the Outbreak Study Group. Clin Infect Dis 2000;31:678–83
5. Ho M, Chen ER, Hsu KH, et al. An epidemic of enterovirus 71 infection in Taiwan. Taiwan Enterovirus Epidemic Working Group. N Engl J Med 1999;341:929–35
6. Yang F, Ren L, Xiong Z, et al. Enterovirus 71 outbreak in the People's Republic of China in 2008. J Clin Microbiol 2009;47:2351–52
7. Ang LW, Koh BK, Chan KP, et al. Epidemiology and control of hand, foot and mouth disease in Singapore, 2001–2007. Ann Acad Med Singapore 2009;38:106–12
8. Hosoya M, Kawasaki Y, Sato M, et al. Genetic diversity of enterovirus 71 associated with hand, foot and mouth disease epidemics in Japan from 1983 to 2003. Pediatr Infect Dis J 2006;25:691–94
9. Mizuta K, Abiko C, Murata T, et al. Frequent importation of enterovirus 71 from surrounding countries into the local community of Yamagata, Japan, between 1998 and 2003. J Clin Microbiol 2005;43:6171–75
10. Podin Y, Gias EL, Ong F, et al. Sentinel surveillance for human enterovirus 71 in Sarawak, Malaysia: Lessons from the first 7 years. BMC Public Health 2006;6:180
11. Sanders SA, Herrero LJ, McPhie K, et al. Molecular epidemiology of enterovirus 71 over two decades in an Australian urban community. Arch Virol 2006;151:1003–13
12. Tran CB, Nguyen HT, Phan HT, et al. The seroprevalence and seroincidence of enterovirus71 infection in infants and children in Ho Chi Minh City, Viet Nam. PLoS One 2011;6:e21116
13. Tu PV, Thao NT, Perera D, et al. Epidemiologic and virologic investigation of hand, foot, and mouth disease, Southern Vietnam, 2005. Emerg Infect Dis 2007;13:1733–41
14. Huang CC, Liu CC, Chang YC, et al. Neurologic complications in children with enterovirus 71 infection. N Engl J Med 1999;341:936–42
15. Lu M, Meng G, He YX, et al. [Pathology of enterovirus 71 infection: An autopsy study of 5 cases]. Zhonghua Bing Li Xue Za Zhi 2009;38:81–85
16. Lum LC, Wong KT, Lam SK, et al. Fatal enterovirus 71 encephalomyelitis. J Pediatr 1998;133:795–98
17. Yang Y, Wang H, Gong E, et al. Neuropathology in 2 cases of fatal enterovirus type 71 infection from a recent epidemic in the People's Republic of China: A histopathologic, immunohistochemical, and reverse transcription polymerase chain reaction study. Hum Pathol 2009;40:1288–95
18. Wong KT, Munisamy B, Ong KC, et al. The distribution of inflammation and virus in human enterovirus 71 encephalomyelitis suggests possible viral spread by neural pathways. J Neuropathol Exp Neurol 2008;67:162–69
19. Wei D, Li KX, Chen E. [Autopsy report of two cases with enterovirus type 71 infection brainstem encephalitis and literature review]. Zhonghua Er Ke Za Zhi 2010;48:220–23
20. Yan JJ, Wang JR, Liu CC, et al. An outbreak of enterovirus 71 infection in Taiwan 1998: A comprehensive pathological, virological, and molecular study on a case of fulminant encephalitis. J Clin Virol 2000;17:13–22
21. Wong KT, Ng KY, Ong KC, et al. Enterovirus 71 encephalomyelitis and Japanese encephalitis can be distinguished by topographic distribution of inflammation and specific intraneuronal detection of viral antigen and RNA. Neuropathol Appl Neurobiol 2012;38:443–53
22. Chen CS, Yao YC, Lin SC, et al. Retrograde axonal transport: A major transmission route of enterovirus 71 in mice. J Virol 2007;81:8996–9003
23. Ong KC, Badmanathan M, Devi S, et al. Pathologic characterization of a murine model of human enterovirus 71 encephalomyelitis. J Neuropathol Exp Neurol 2008;67:532–42
24. Baker AB. Poliomyelitis. 16. A study of pulmonary edema. Neurology 1957;7:743–51
25. Fu YC, Chi CS, Chiu YT, et al. Cardiac complications of enterovirus rhombencephalitis. Arch Dis Child 2004;89:368–73
26. Shang L, Xu M, Yin Z. Antiviral drug discovery for the treatment of enterovirus 71 infections. Antiviral Res 2013;97:183–94
27. Zhu FC, Meng FY, Li JX, et al. Efficacy, safety, and immunology of an inactivated alum-adjuvant enterovirus 71 vaccine in children in China: A multicentre, randomised, double-blind, placebo-controlled, phase 3 trial. Lancet 2013;381:2024–32
28. Chang GH, Luo YJ, Wu XY, et al. Monoclonal antibody induced with inactived EV71-Hn2 virus protects mice against lethal EV71-Hn2 virus infection. Virol J 2010;7:106
29. Foo DG, Alonso S, Chow VT, et al. Passive protection against lethal enterovirus 71 infection in newborn mice by neutralizing antibodies elicited by a synthetic peptide. Microbes Infect 2007;9:1299–306
30. Liou JF, Chang CW, Tailiu JJ, et al. Passive protection effect of chicken egg yolk immunoglobulins on enterovirus 71 infected mice. Vaccine 2010;28:8189–96
31. Ong KC, Devi S, Cardosa MJ, et al. Formaldehyde-inactivated whole-virus vaccine protects a murine model of enterovirus 71 encephalomyelitis against disease. J Virol 2010;84:661–65
32. Abzug MJ, Keyserling HL, Lee ML, et al. Neonatal enterovirus infection: Virology, serology, and effects of intravenous immune globulin. Clin Infect Dis 1995;20:1201–6

33. Johnston JM, Overall JC Jr. Intravenous immunoglobulin in disseminated neonatal echovirus 11 infection. Pediatr Infect Dis J 1989;8:254–56
34. McKinney RE Jr, Katz SL, Wilfert CM. Chronic enteroviral meningoencephalitis in agammaglobulinemic patients. Rev Infect Dis 1987;9:334–56
35. Pasic S, Jankovic B, Abinun M, et al. Intravenous immunoglobulin prophylaxis in an echovirus 6 and echovirus 4 nursery outbreak. Pediatr Infect Dis J 1997;16:718–20
36. Valduss D, Murray DL, Karna P, et al. Use of intravenous immunoglobulin in twin neonates with disseminated coxsackie B1 infection. Clin Pediatr (Phila) 1993;32:561–63
37. Wang SM, Liu CC. Enterovirus 71: Epidemiology, pathogenesis and management. Expert Rev Anti Infect Ther 2009;7:735–42
38. Dalton KP, Ringleb F, Martin Alonso JM, et al. Rapid purification of myxoma virus DNA. J Virol Methods 2009;162:284–87
39. Conn PM, SpringerLink. *Neuroscience in Medicine*. 3rd Ed. Totowa, NJ: Humana Press, 2008
40. Heimer L. *The Human Brain and Spinal Cord: Functional Neuroanatomy and Dissection Guide*. 2nd Ed. New York, NY: Springer, 1995
41. Wilson-Pauwels L, Akesson EJ, Stewart PA. *Cranial Nerves: In Health and Disease*. 2nd Ed. Hamilton, Ont. London: BC Decker, 2002
42. Fu YC, Chi CS, Lin NN, et al. Comparison of heart failure in children with enterovirus 71 rhombencephalitis and cats with norepinephrine cardiotoxicity. Pediatr Cardiol 2006;27:577–84
43. Hoff JT, Nishimura M, Garcia-Uria J, et al. Experimental neurogenic pulmonary edema. Part 1: The role of systemic hypertension. J Neurosurg 1981;54:627–31
44. Kao SJ, Yang FL, Hsu YH, et al. Mechanism of fulminant pulmonary edema caused by enterovirus 71. Clin Infect Dis 2004;38:1784–88
45. He Y, Ong KC, Gao Z, et al. Tonsillar crypt epithelium is an important extra-central nervous system site for viral replication in EV71 encephalomyelitis. Am J Pathol 2014;184:714–20
46. Lin TY, Chang LY, Huang YC, et al. Different proinflammatory reactions in fatal and non-fatal enterovirus 71 infections: Implications for early recognition and therapy. Acta Paediatr 2002;91:632–35
47. Wang SM, Lei HY, Huang KJ, et al. Pathogenesis of enterovirus 71 brainstem encephalitis in pediatric patients: Roles of cytokines and cellular immune activation in patients with pulmonary edema. J Infect Dis 2003; 188:564–70
48. Wang SM, Lei HY, Liu CC. Cytokine immunopathogenesis of enterovirus 71 brain stem encephalitis. Clin Dev Immunol 2012;2012:876241
49. Wang YF, Yu CK. Animal models of enterovirus 71 infection: Applications and limitations. J Biomed Sci 2014;21:31
50. Yu CK, Chen CC, Chen CL, et al. Neutralizing antibody provided protection against enterovirus type 71 lethal challenge in neonatal mice. J Biomed Sci 2000;7:523–28
51. Wang JN, Yao CT, Yeh CN, et al. Critical management in patients with severe enterovirus 71 infection. Pediatr Int 2006;48:250–56
52. Wang SM, Liu CC, Tseng HW, et al. Clinical spectrum of enterovirus 71 infection in children in southern Taiwan, with an emphasis on neurological complications. Clin Infect Dis 1999;29:184–90
53. de Vries HE, Kuiper J, de Boer AG, et al. The blood-brain barrier in neuroinflammatory diseases. Pharmacol Rev 1997;49:143–55
54. Engelhardt B. Development of the blood-brain barrier. Cell Tissue Res 2003;314:119–29
55. Kniesel U, Risau W, Wolburg H. Development of blood-brain barrier tight junctions in the rat cortex. Brain Res Dev Brain Res 1996;96:229–40
56. Collins FM. Vaccines and cell-mediated immunity. Bacteriol Rev 1974; 38:371–402
57. Cao RY, Dong DY, Liu RJ, et al. Human IgG subclasses against enterovirus Type 71: Neutralization versus antibody dependent enhancement of infection. PLoS One 2013;8:e64024
58. Chen IC, Wang SM, Yu CK, et al. Subneutralizing antibodies to enterovirus 71 induce antibody-dependent enhancement of infection in newborn mice. Med Microbiol Immunol 2013;202:259–65
59. Fujii K, Nagata N, Sato Y, et al. Transgenic mouse model for the study of enterovirus 71 neuropathogenesis. Proc Natl Acad Sci U S A 2013; 110:14753–58
60. Lin YW, Yu SL, Shao HY, et al. Human SCARB2 transgenic mice as an infectious animal model for enterovirus 71. PLoS One 2013;8:e57591